Intercalation and Exfoliation Behavior of Epoxy Resin/Curing Agent/Montmorillonite Nanocomposite

WEI-BING XU,[1,2] SU-PING BAO,[2] PING-SHENG HE[1]*

[1] Department of Polymer Science and Engineering, University of Science and Technology of China, Hefei 230026, Anhui, People's Republic of China

[2] Department of Polymer Science and Engineering, Hefei University of Technology, Hefei 230009, Anhui, People's Republic of China

Received 19 December 2000; accepted 10 August 2001

ABSTRACT: The epoxy resin/curing agent/montmorillonite nanocomposite was prepared by a casting and curing process. The intercalation and exfoliation behaviors of epoxy resin in the presence of organophilic montmorillonite were investigated by X-ray diffraction (XRD) and dynamic mechanical thermal analysis (DMTA). For the diethylenetriamine curing agent, the intercalated nanocomposite was obtained; and the exfoliated nanocomposite would be formed for tung oil anhydride curing agent. The curing condition does not affect the resulting kind of composite, both intercalation or exfoliation. For intercalated nanocomposite, the glass transition temperature T_g, measured by DMTA and affected by the curing temperature of matrix epoxy resin is corresponded to that of epoxy resin without a gallery. The α' peak of the loss tangent will disappear if adding montmorillonite into the composite. It was also found that the T_g of the exfoliated nanocomposite decreases with increasing montmorillonite loading. © 2002 John Wiley & Sons, Inc. J Appl Polym Sci 84: 842–849, 2002; DOI 10.1002/app.10354

Key words: resin; clay; nanocomposites; X-ray; glass transition

INTRODUCTION

Nanocomposite is a composite in which inorganic filler is dispersed within the resin matrix in a nanometer scale. One approach to preparing the nanocomposite is *in situ* polymerization of monomer immersed into layered clay. In general, the dispersion of clay particles in the resin matrix can result in the formation of three general types of composite:[1] (a) normal composites; (b) intercalated nanocomposites: it is formed by the insertion of polymer molecules into the clay host galleries and the clay remains a regular gallery structure, although the basal spacing rises; (c) exfoliated nanocomposite: the individual 10 Å-thick silicate layers are dispersed in the resin matrix and segregated from one another, and the gallery structures are completely destroyed. Both intercalated and exfoliated nanocomposites offered some special physical and mechanical properties compared to the normal composites, and some nanocomposites such as PA/clay,[2–4] PS/clay,[5,6] PMMA/clay,[7] PP/clay,[8] and PU/clay[9] have been produced in the lab and in industry in recent years.

Nowadays, a lot of scientists are paying great attention to the layer silicate–epoxy nanocomposite.

Giannelis[10] prepared an exfoliated layer silicate-epoxy nanocomposite from diglycidyl ether of bisphenol A and a nadic methyl anhydride curing

Correspondence to: P.-S. He.

Contract grant sponsor: Nature Science Foundation of Anhui Province, China.

Journal of Applied Polymer Science, Vol. 84, 842–849 (2002)

agent, and found that the dynamic storage modulus of the nanocomposite containing 4 vol % silicate was approximately 58% higher in glassy region and 450% higher in the rubbery plateau region compared to the pristine polymer. Monolithic epoxy exfoliated clay nanocomposites were prepared from the reaction of alkylammonium-exchanged smectite clays with diglycidyl ether of bisphenol A and an *m*-phenylenediamine curing agent by Pinnavaia.[11–13] He proposed that there were intergallery polymerization and extragallery polymerization during cure of epoxy–clay mixture. When the rate of extragallery polymerization was larger than that of the intergallery polymerization, the intercalated nanocomposite was obtained. The exfoliated nanocomposite was obtained when the two rates were matching. It was also found that intragallery polymerization and clay layer exfoliation could be regulated in part by selecting hydrophobic alkylammonium exchanged cations that were sufficiently acidic to catalyze the polymerization process. However, for the cure process of thermosets, the effect of the type of curing agent on the formation process of the epoxy–clay nanocomposite has not yet been investigated.

In this presentation, the nanocomposite was prepared by mixing epoxy resin with a desired amount of clay exchanged with alkylammonium bromide with curing agents of diethylenetriamine or tung oil anhydride. Emphasis was concentrated on the intercalation and exfoliation behavior of clay and DMTA of the resulting nanocomposites. It was found that the intercalated or exfoliated nanocomposites could be produced by changing the curing agent.

EXPERIMENTAL

Materials

Na^+-Montmorillonite, the cation exchange capacity (CEC) value of 100 mmol/100 g, was provided by Qingshan Chemistry Agent Factory, Lin'an, China. The diglycidyl ether of biphenyl A, epoxy resin E-51, was obtained from Shanghai Resin Factory. Diethylenetriamine (DETA) with a molecular weight of 364.46 was obtained from the 14th Dye Factory, Shanghai. Tung oil anhydride (TOA) and tri (dimethylamino-methyl) phenol (DMP-30) were generously provided by the Corporation of Hefei Baofeng Chemistry. The surfactant of clay, $CH_3(CH_2)_{15}N(CH_3)_3Br$, was purchased from the Research Institute of Xinhua Active Material in Changzhou.

Ion Exchanged Clays

Na^+-Montmorillonite was added to a three-neck 1000 mL round-bottom flask loaded with distilled water, and mixed using a mechanical stirrer equipped with a glass stirring rod in room temperature, 30 g $CH_3(CH_2)_{15}N(CH_3)_3Br$ per hundred grams clay by weight was added and placed in a 90°C water bath for 2 h. The exchanged clays were washed with deionized water until no bromide was detected with 0.1 *N* $AgNO_3$ solution and dried in the air. The clays were ground with a mortar and pestle, and the 40–60-μm fraction was collected. The product made in this way was identified as 16-Mont.

Sample Preparation

Epoxy/organophilic montmorillonite/curing agent mixtures were obtained and poured into a PTFE [poly(tetrafluoroethylene)] mold. After they were cast into small bars, they were degassed simultaneously. For the diethylenetriamine curing agent, another method was used. Epoxy resin was solvated with organophilic montmorillonite at 80°C for 72 h. The monomer of epoxy resin entered into the gallery of clay. Finally, they were cast into small bars and degassed.

Measurement and Characterization

The lattice spacing of montmorillonite was measured by Rigaku D/max-γB rotating anionod X-ray diffractometer with Cu Kα line (λ = 1.5418 Å), a tube voltage of 40 kV, and tube current of 100 mA. The scanning range is from 2.2° to 10° (or 2.5° to 30°) with a rate of 2°/min. A dynamic mechanical thermal analyzer (DMTA IV) was used in characterizing the viscoelastic behavior of resin matrix. The measurement was carried out at a rate of 5°C/min, frequency of 1.1 Hz and strain of 0.01%, giving Young's storage modulus E', loss modulus E'' and loss tangent tan δ. The specimen with the width 3–5 mm, length 15–25 mm, and thickness 1–4 mm, depending on the sample used.

RESULTS AND DISCUSSION

Preparation of Organophilic Clay

Na^+-Montmorillonite is composed of sodium ions and negative montmorillonite. It disperses homo-

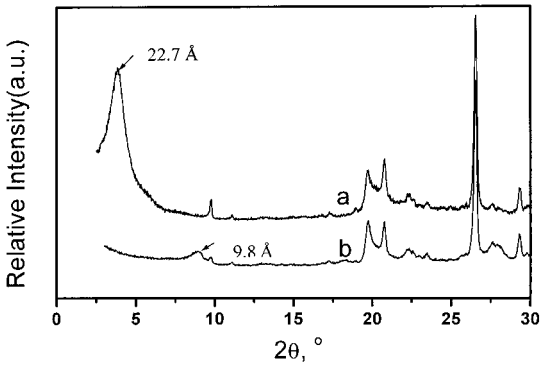

Figure 1 XRD patterns of inorganic montmorillonite and the organoclay 16-Mont (a) the organoclay 16-Mont, (b) inorganic montmorillonite.

geneously in water, but does not disperse in organic solvent. When specific ammonium, for example, $CH_3(CH_2)_{15}N(CH_3)_3Br$ is chosen as the intercalating reagent, the lattice spacing of clay rises and the hydrophilicity of montmorillonite is reduced to allow dispersion in organic solvent, and it is convenient that the monomer of the epoxy resin entered into the gallery of organophilic montmorillonite.

Figure 1 shows the X-ray diffraction patterns of inorganic montmorillonite and the organoclay 16-Mont in the 2θ region of 2.5–30°. There is a peak at $2\theta = 9°$ for inorganic montmorillonite, but the peak appears at $2\theta = 3.88°$ for the organoclay 16-Mont, which is assigned to the (001) lattice spacing of montmorillonite. The lattice spacing corresponds to an interlayer spacing of organophilic montmorillonite. Therefore, the interlayer spacing of inorganic montmorillonite and the organoclay 16-Mont is 9.8 and 22.7 Å, respectively, according to $2d\sin\theta = n\ \lambda$.

X-ray Diffraction Analysis

In this study, predetermined amounts of organophilic montmorillonite were added into the epoxy resin system. The 16-Mont loading varied from 0 to 10%. XRD patterns for the epoxy resin/clay/DETA composite with different organoclay loading cured at 70°C for 2 h are shown in Figure 2. Compared to that of the 16-Mont, the (001) peak shifted to the lower angle, and the intensity of the peak increased with increasing organophilic montmorillonite loading. The peak of 16-Mont ($2\theta = 3.88°$) has disappeared; the first and second diffraction peaks appeared at $2\theta = 2.56°$ and 5°, respectively, indicating that the intercalated

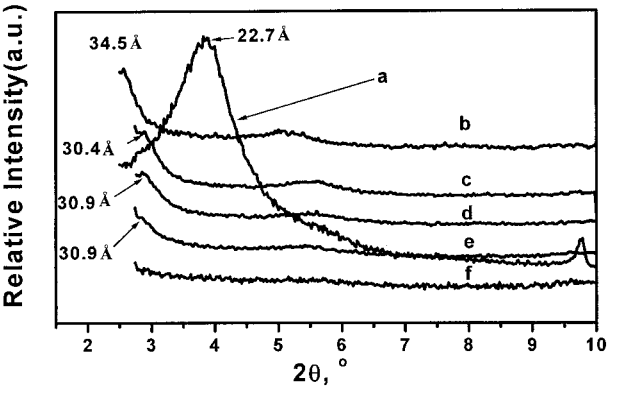

Figure 2 XRD patterns of the organoclay 16-Mont and 16-Mont/DETA/EP hybrids: (a) 16-Mont; (b) 10% 16-Mont/DETA/EP hybrid; (c) 7% 16-Mont/DETA/EP hybrid; (d) 5% 16-Mont/DETA/EP hybrid; (e) 3% 16-Mont/DETA/EP hybrid; (f) 0% 16-Mont/DETA/EP hybrid.

nanocomposite with the lattice spacing of 30.9–34.5 Å was obtained.

Prior to curing with diethylenetriamine, the epoxy resin was solvated with 10% organoclay at 80°C for 72 h. Figure 3 shows the X-ray diffraction patterns of epoxy swollen clay/DETA nanocomposite and epoxy-unsolvated clay/DETA nanocomposite cured in different conditions. The results reveal that varying the curing condition has little or no effect on the clay basal spacing. At the same curing temperature [70°C (2 h) 120°C (2 h)], there are a little change of the two diffraction patterns for epoxy-solvated clay and epoxy-unsolvated clay, which exhibit evident Bragg diffrac-

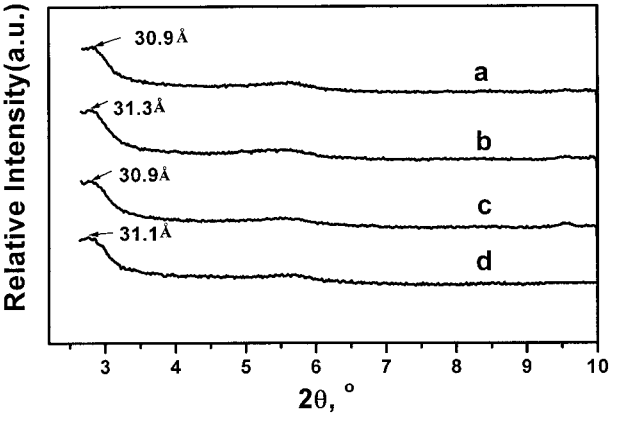

Figure 3 XRD patterns of epoxy-swollen clay/DETA nanocomposites cured at different conditions: (a) 140°C, 2 h; (b) 120°C, 3 h; (c) 70°C, 2 h, 120°C, 2 h; (d) 70°C, 2 h, 120°C, 2 h (unswollen).

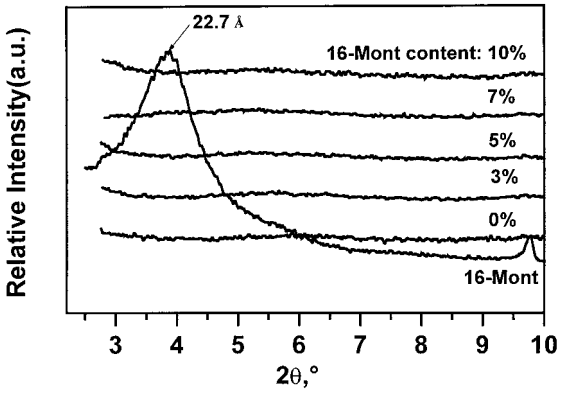

Figure 4 XRD patterns of the organoclay 16-Mont and 16-Mont/epoxy/TOA/DMP-30 nanocomposites.

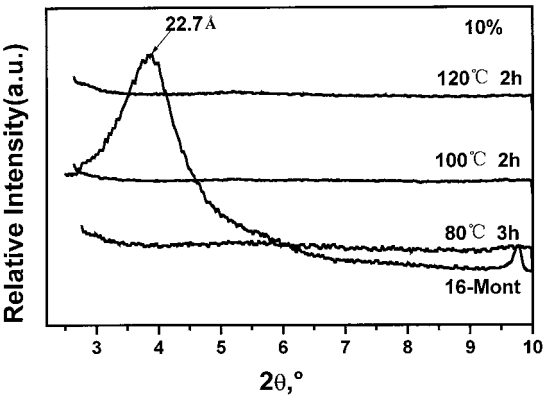

Figure 5 XRD patterns of 5% 16-Mont/EP/TOA/DMP-30 nanocomposite cured at different conditions.

tion peaks at 31.1 and 30.9 Å, respectively, and in Figure 3, composites cured at 120°C (3 h) and 140°C (2 h) exhibit evident Bragg diffraction peaks at 31.3 and 30.9 Å, respectively. So the position of diffraction peak also changes a little with the change of curing temperature. Although the course of swelling can ensure the contact of epoxy resin and 16-Mont, the amount of resin that can be loaded into galleries of organoclay is at a limit. Qi[14] also found that it was easy for epoxy molecules to penetrate into the clay basal spacing, and the clay would be saturated with the epoxy molecules to some degree.

Figure 4 shows XRD diffraction patterns for the EP/clay/TOA/DMP-30 nanocomposite containing various clay loadings with the results of 16-Mont for comparison. There is no diffraction peak at 2θ = 2.5–2.6° even at 2θ = 5° for the composite cured with TOA, indicating that the clay was exfoliated without regular repeat distance between the layers. It is considered that the cure reaction occurs at high temperature for tung oil anhydride curing agent; a large amount of epoxy monomer can enter into the gallery and the intragallery polymerization can be occurred at a comparable rate to extragallery polymerization. Consequently, the galleries continue to expand when the degree of polymerization increases and an exfoliated nanocomposite is formed. To form the intercalated nanocomposite, the rate of intragallery polymerization should not be much larger than that of extragallery polymerization. The lattice spacing of intercalated nanocomposite increases, but there are diffraction peaks in the X-ray diffraction pattern of the intercalated nanocomposite. If the lattice spacing increases further, the diffraction peak will disappear, indicating that the exfoliated nanocomposite is obtained. And every clay loading can all form exfoliated nanocomposites. Even when the clay loadings increase, the rate of extragallery polymerization allows a sufficient amount of epoxy resin molecules penetrate the gallery space, and intergallery polymerization can occur at a similar rate. Thus, exfoliated nanocomposites can be obtained by controlling the rates of intergallery polymerization and extragallery polymerization.

To verify the importance of curing temperature on exfoliation, XRD patterns for crosslinked epoxy–clay–TOA–DMP-30 composites containing 5 and 10% 16-Mont cured under different thermal conditions are shown in Figures 5 and 6, respectively.

From the Figures 5 and 6, the absence of Bragg diffraction indicated that the clay tactoids have been completely exfoliated, and the different cur-

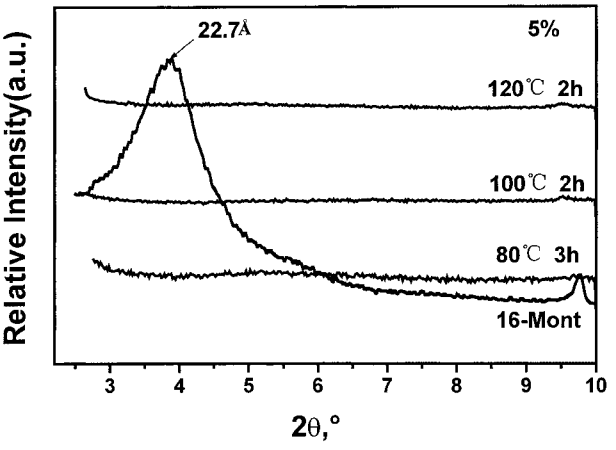

Figure 6 XRD patterns of 10% 16-Mont/epoxy/TOA/DMP-30 nanocomposites cured at different conditions.

ing temperature resulted in little or no change in the clay basal spacing. Pinnavaia[1] proposed that it is crucial to select curing conditions that balance the intra- and extragallery polymerization rates in obtaining the exfoliated nanocomposite. In this article, as the curing rate of tung oil anhydride in inter- and extragallery is low, a large quantity of the monomer of epoxy resin entered into the galleries, and it leads to the similar rate of inter- and extragallery polymerization.

Dynamic Mechanical Thermal Analysis (DMTA)

Some mechanical properties and the glass transition temperature T_g of intercalated and exfoliated nanocomposite may be distinguished by the dynamic mechanical thermal analysis. The curves of storage modulus E' of EP/16-Mont/DETA nanocomposites with different clay loadings (0, 3, 5, and 10%, respectively, and all cured at 70°C for 2 h) were shown in Figure 7. The 16-Mont loading affected on the position of interval friction peak. The T_g of nanocomposite with 3% 16-Mont loading decreased comparing to pure epoxy resin, but when the 16-Mont loading being up to 5 or 10%, the T_g changed a little. This is due to the difference between the intragallery polymerization and the extragallery polymerization. Owing to the spatially restricted nature of the intragallery epoxy resin, one might be not able to measure the T_g of the intragallery epoxy resin in the range of measurement. Winey[5] found by DSC that a diminishing of the T_g of polystyrene with intercalation, leading to a complete absence of the T_g trace when all polymer in the composite has been intercalated. Giannelis[15] also found that the motions of the intercalated PEO chains are inherently noncooperative relative to the cooperative

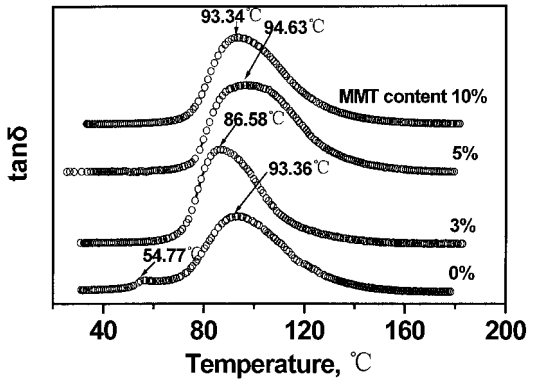

Figure 7 Loss tangent of 16-Mont/epoxy/DETA nanocomposite with different 16-Mont content.

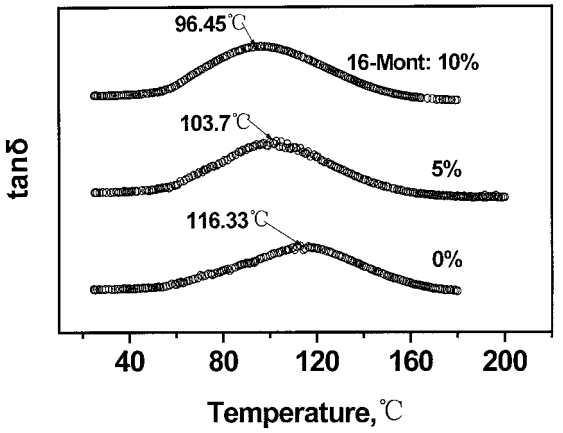

Figure 8 Loss tangent of 16-Mont/epoxy/TOA/DMP-30 nanocomposite at different 16-Mont content.

T_g motions in the amorphous portion of the bulk polymer, in line with the result of DMTA here. So the interval frictions of composite correspond to the T_g of epoxy resin without the gallery. In addition, for the pure epoxy, the position of α' relaxation peak is at 54°C, while for the epoxy/clay nanocomposite, the peak disappears, signifying that the uniformity of the material can be improved due to the addition of 16-Mont.

To compare the effect of different curing agent, Figure 8 showed the DMTA results of EP/TOA/DMP-30/16-Mont cured at 100°C for 2 h. With increasing organoclay loadings, the T_g of the nanocomposite tends to decrease, which may be associated with the void of crosslinking in the hybrid. When the organoclay was added into the epoxy, the free volume of highly cured epoxy is increased; the segmental mobility within the polymer increases, leading to the lower T_g.

The effect of the curing temperature on the T_g of the intercalated nanocomposite and the exfoliated nanocomposite is different, as shown in Figures 9 and 10. For the intercalated nanocomposite (Fig. 9), the T_g mainly changed with the curing temperature and curing time. If the curing temperature becomes higher or the curing time becomes longer, the process of crosslinking becomes easier, the free volume out of the gallery is reduced, and the segmental mobility within polymer out of the gallery decreased. Thus, we can think it true that the T_g obtained by DMTA is the glass transition temperature of extragallery polymer.

For exfoliated nanocomposite, as shown in Figure 10, the different T_g occurred for the samples under different curing conditions. When the cur-

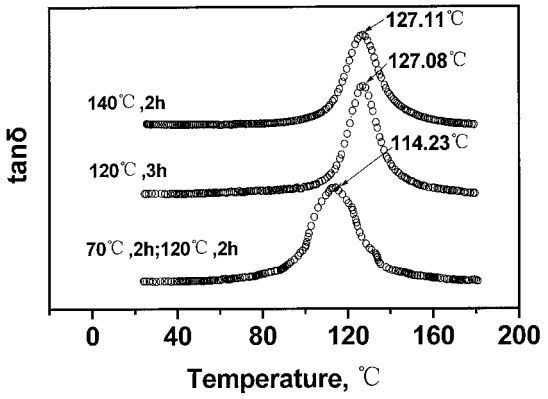

Figure 9 Loss tangent of 10% 16-Mont/solvated epoxy/DETA nanocomposite cured at different conditions.

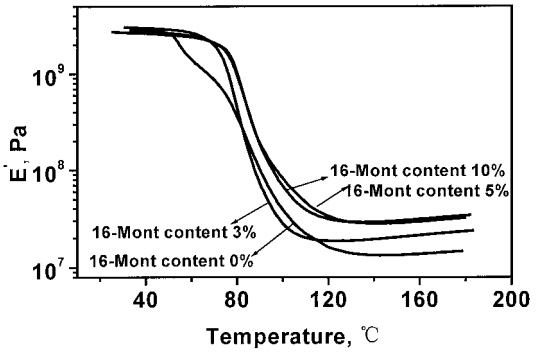

Figure 11 Storage modulus of 16-Mont/EP/DETA nanocomposites at different 16-Mont content.

ing time is the same, we have investigated that the effect of curing temperature on T_g. Obviously, the T_g of hybrid cured at the higher temperature (120°C) is higher than that of hybrid cured at the lower temperature (100°C). On the basis of the viewpoint above in the X-ray analysis, the organoclay dispersed in exfoliated nanocomposite irregularly. The improvement of curing temperature raises the crosslinking density of intra- and extragallery and the increase of the glass transition temperature is formed. The crosslinking density decreased with the degradation of the curing temperature, but the longer the curing time, the higher the crosslinking density which formed during the process of curing, can result in the improvement of the T_g of nanocomposite. Therefore, the T_g cured under 80°C (3 h) is larger than the T_g cured under 100°C (2 h).

Of course, the change of storage modulus of hybrids could be also observed. As shown in Figure 11, for the epoxy resin/clay/DETA intercalation nanocomposite, it may be confirmed that the amplitude of storage modulus in the rubbery plateau region increases with increasing the 16-Mont loading. This is due to the reinforcement of the clay gallery, as expected.

In the DMTA process of the exfoliated nanocomposite, it could be found that the different contents of 16-Mont correspond to the similar amplitude of storage modulus in the rubbery plateau region. In Figure 12, it is evidently observed that the storage modulus, which corresponds to the same temperature in the glass transition region, decreased with increasing organoclay loading. In the exfoliated nanocomposite, it is considered that the organoclay is dispersed into the epoxy system irregularly and the void of the crosslinking is increased. Then the segmental mobility raises, which leads to the decrease of the storage modulus at the same temperature. But at the same time, the reinforcement of the monolithic structure of the organoclay leads to the increase of the storage modulus at the same temperature.

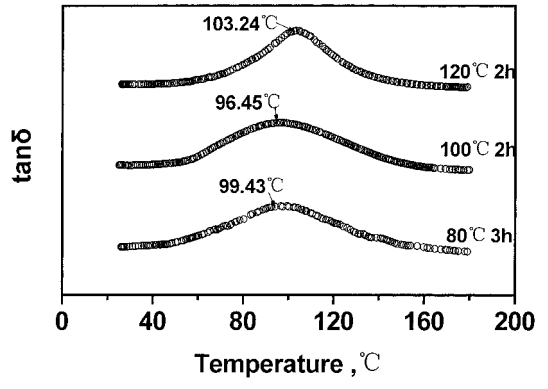

Figure 10 Loss tangent of 10% 16-Mont/epoxy/TOA/DMP-30 nanocomposites cured at different conditions.

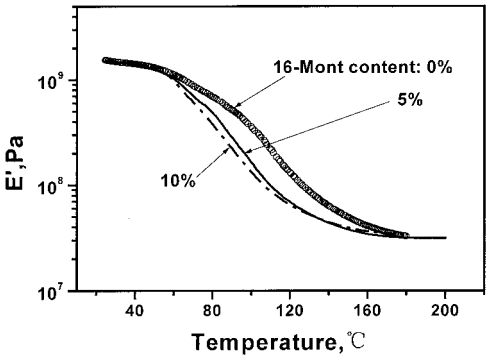

Figure 12 Storage modulus of 16-Mont/epoxy/TOA/DMP-30 nanocomposites with different 16-Mont content.

So these two factors result in a tendency to change the storage modulus, as shown in Figure 12.

As described above, the swelling of the clay by the epoxy monomer does not change the type of the nanocomposite, and the change of storage modulus is illustrated in Figure 13. The change of storage modulus of the composite cured at the lower temperature is larger than that cured at the higher temperature in the glassy region. In the range of the temperature (80–120°C), the change of the storage modulus of the 10% 16-Mont/epoxy/TOA/DMP-30 nanocomposite is shown in Figure 14. It is found that the storage modulus, which corresponds to the same temperature, increased with the increase of the curing temperature. This can be explained that the change of the crosslinking density leads to the result. For the exfoliated nanocomposite, because of the same content of the clay, the segment of the epoxy that existed in the organoclay is similar, and the higher curing temperature results in the improvement of the crosslink density.

CONCLUSION

Organophilic montmorillonite is obtained by the ion exchange of organic ammonium compound, and its interlayer space changes from 9.8 to 22.7 Å. The epoxy resin/curing agent/montmorillonite nanocomposite is prepared by a casting and curing process, and the intercalation and exfoliation behaviors of epoxy resin in the presence of organophilic montmorillonite are investigated by X-ray diffraction and dynamic mechanical thermal analysis. It proves that different types of nanocomposites can be reached if a different curing agent is added. The addition of the diethylenetriamine curing agent, epoxy resin intercalates into the clay galleries and the intercalated nanocomposite is obtained; with addition of the tung oil anhydride curing agent, the distance of the clay gallery rises and the exfoliated nanocomposite is formed, and the change of curing condition does not change the effect of intercalation or exfoliation. For the intercalated nanocomposite, the glass transition temperature of epoxy corresponds to the epoxy resin cured out of the gallery from the result of the DMTA, which is affected by the curing temperature and time, and the α' peak of the loss tangent of the nanocomposite disappears with addition of montmorillonite. DMTA proves that the glass transition temperature of the exfoliated nanocomposite decreases with the increase of the montmorillonite content, the storage modulus in the rubbery region increases with the increase of the montmorillonite content, and the amplitude of the storage modulus of the intercalated nanocomposite in the rubbery plateau region increases with increasing the 16-Mont loading.

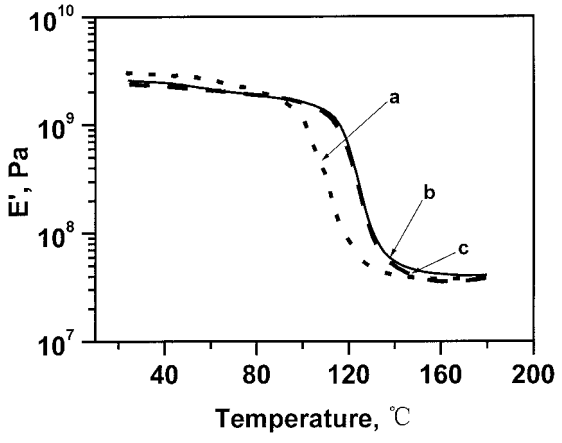

Figure 13 Storage modulus of 16-Mont/solvated EP/DETA hybrids cured at different conditions: (a) 70°C, 2 h; 120°C, 2 h; (b) 120°C, 3 h; (c) 140°C, 2 h.

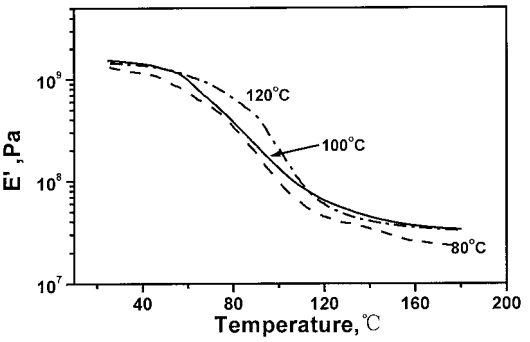

Figure 14 Storage modulus of 16-Mont/EP/TOA/DMP-30 hybrids at different curing temperatures.

The authors gratefully acknowledge the financial support from the Nature Science Foundation of Anhui Province, China, and also thank the College of Chemical Engineering of Anhui University for the partial measurement support of this research.

REFERENCES

1. Lan, T.; Kaviratna, P. D.; Pinnavaia, T. J. Chem Mater 1995, 7, 2144.

2. Usuki, A.; Kojima, Y.; Kawasumi, M.; Kamigaito, O. J Mater Res 1993, 8, 1179.
3. Kojima, Y.; Usuki, A.; Kawasumi, M.; Kamigaito, O. J Polym Sci Part A Polym Chem 1993, 31, 1755.
4. Liu, L.; Qi, Z.; Zhu, X. J Appl Polym Sci 1999, 71, 1133.
5. Sikka, M.; Cerini, L. N.; Ghosh, S. S.; Winey, K. I. J Polym Sci Part B Polym Phys 1996, 34, 1443.
6. Vaia, R. A.; Giannelis, E. P. Macromolecules 1997, 30, 8000.
7. Lee, D. C.; Jang, L. W. J Appl Polym Sci 1996, 61, 1117.
8. Xu, W. B.; Ge, M. L.; He, P. S. China Plastics (in Chinese) 2000, 14, 27.
9. Chen, T. K.; Tien, Y. I.; Wei, K. H. J Polym Sci Part A Polym Chem 1999, 37, 2225.
10. Messersmith, P. B.; Giannelis, E. P. Chem Mater 1994, 6, 1719.
11. Pinnavaia, T. J.; Lan, T.; Kaviratna, P. D. Proc ACS Div Polym Mater Sci Eng (PMSE) 1995, 73, 117.
12. Lan, T.; Pinnavaia, T. J. Chem Mater 1994, 6, 2216.
13. Lan, T.; Kaviratna, P. D.; Pinnavaia, T. J. Proc ACS Div Polym Mater Sci Eng (PMSE) 1994, 71, 527.
14. Lu, J.; Yi, X.; Qi, Z. Polym Bull 2000, 2, 24.
15. Vaia, R. A.; Sauer, B. B.; Tse, O. K.; Giannelis, E. P. J Polym Sci Part B Polym Phys 1997, 35, 59.